UNIVERSITY OF PATRAS

ERASMUS+ 2025

Iron & manganese deposits and Earth evolution

Harilaos ("Harry") Tsikos

Applied & Environmental Geochemistry

Fe and Mn in the context of Earth evolution

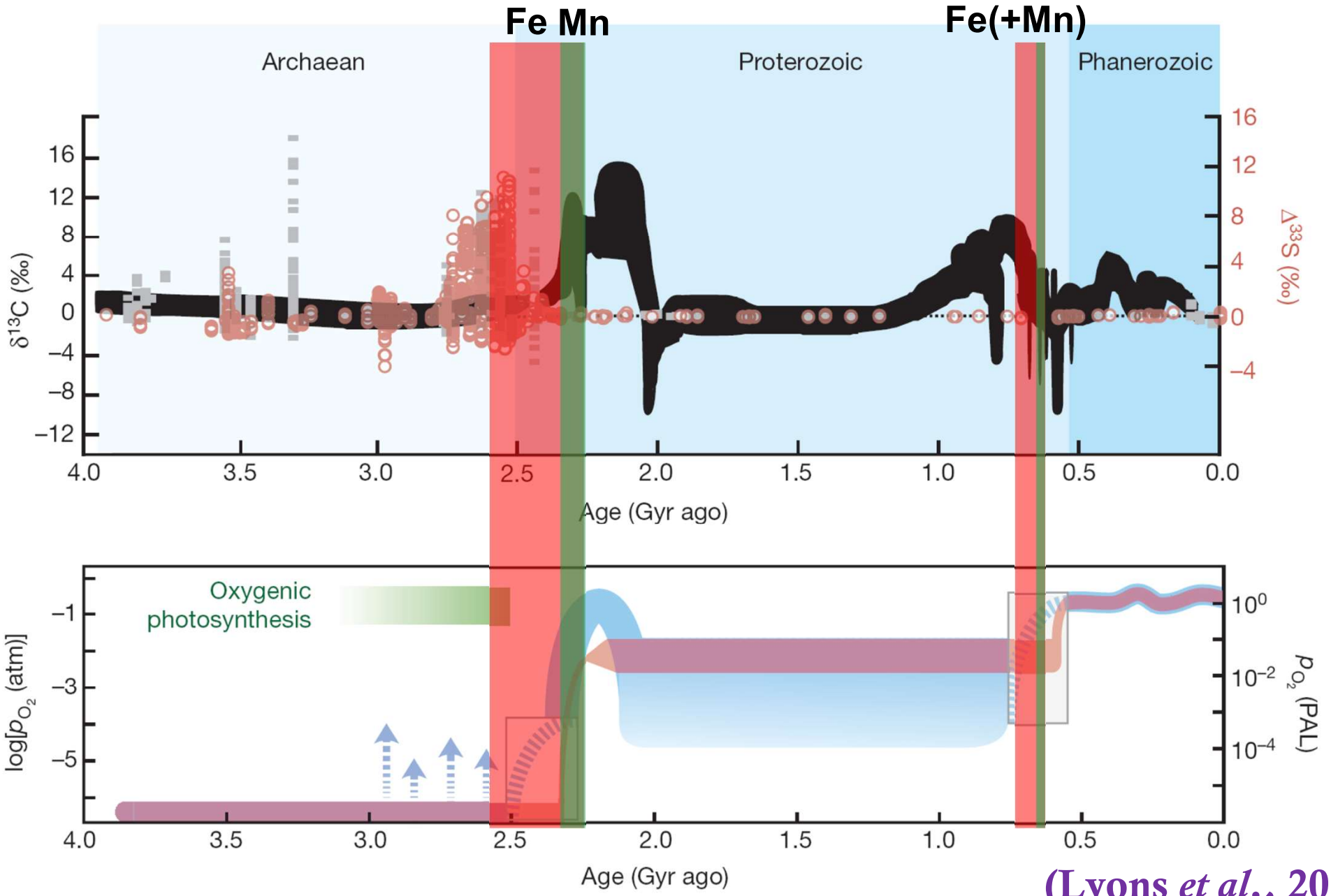

(Lyons *et al.*, 2014)

Early Earth History in a nutshell

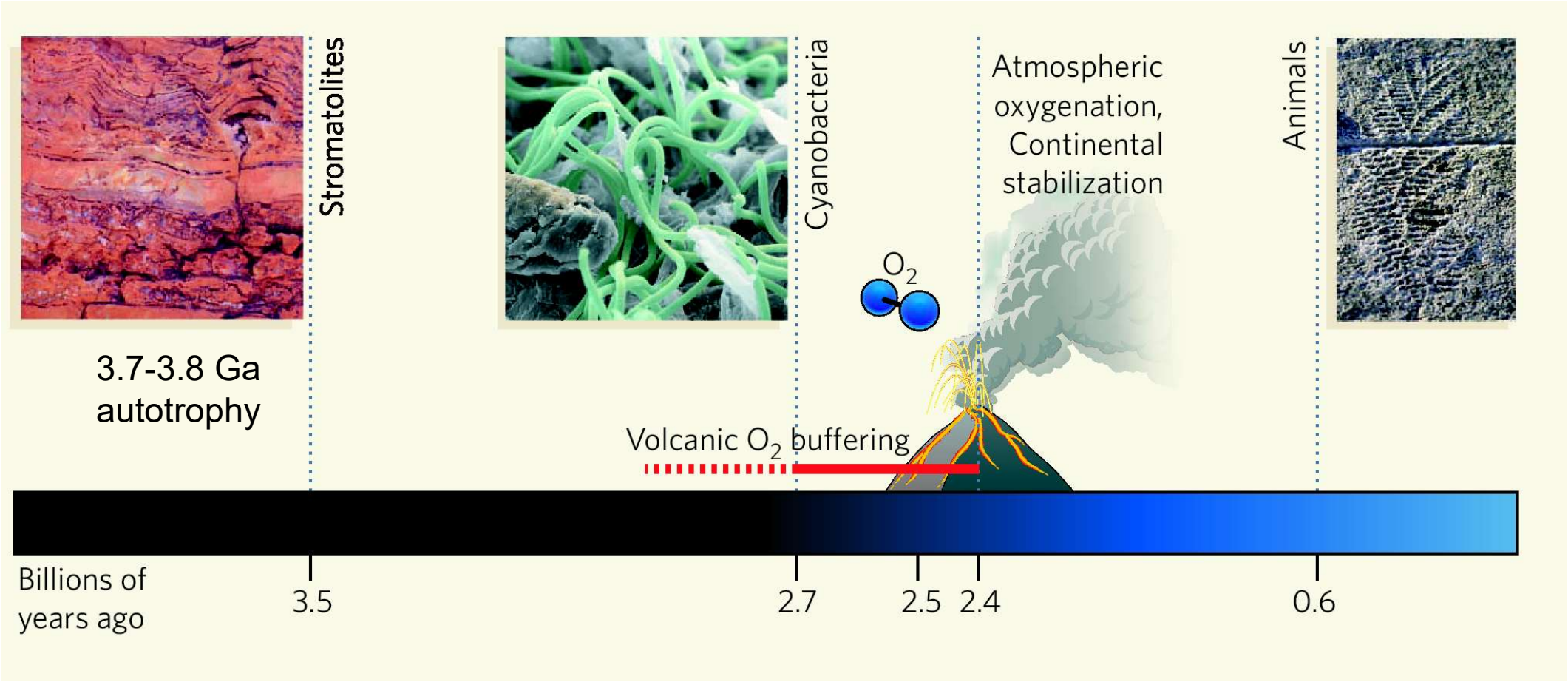

(Kump & Barley, 2007; Lyons, 2007)

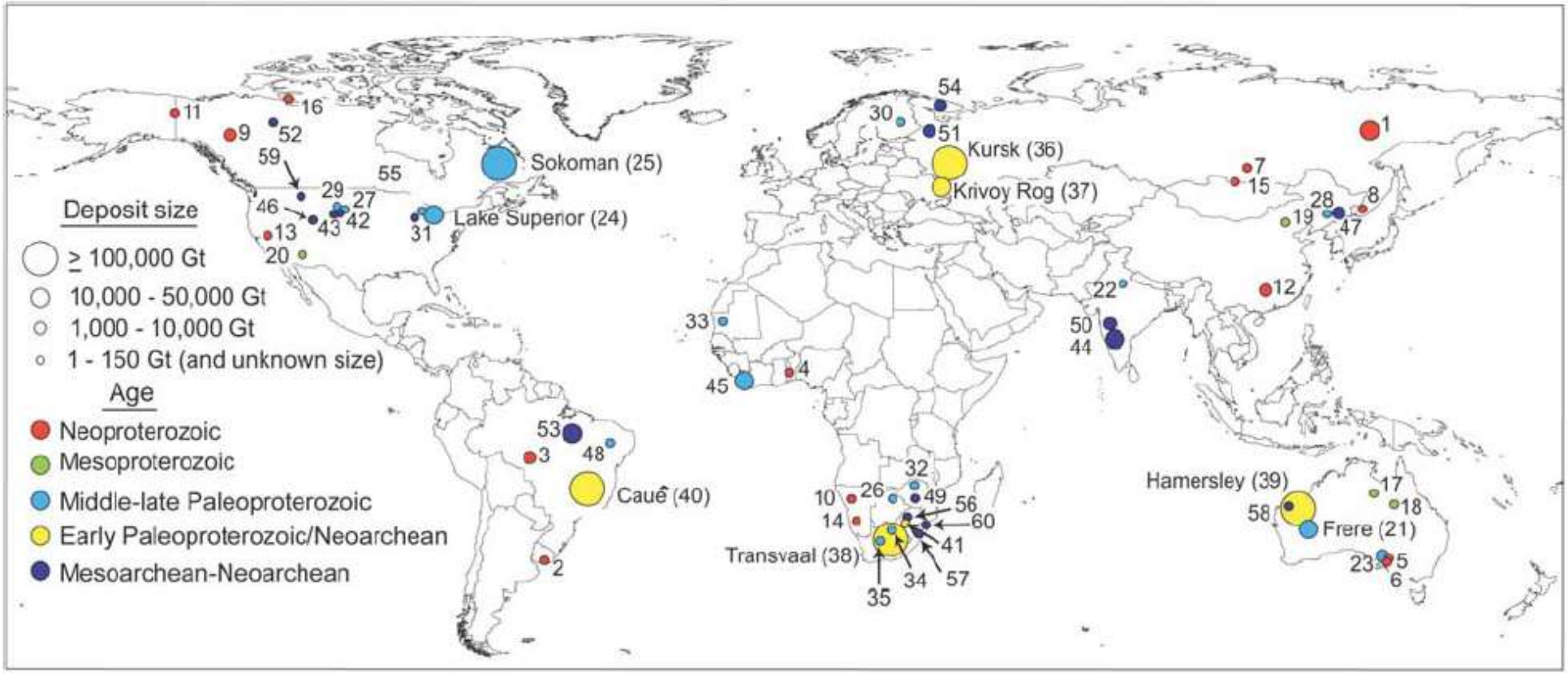

Major sediment-hosted iron formations of the world, including BIF, GIF, and Rapitan-type iron formations. Also shown are several ironstones. Iron deposits are distinguished on the basis of size and age. Key to numbered iron-rich sedimentary units and areas (see App. 1 and text for information on age constraints and on stratigraphic and geographic position): 1 = Maly Khinghan Formation, 2 = Yerbel Formation, 3 = Jacadigo Group, 4 = Bisokpabe Group, 5 = Holowilena Ironstone, 6 = Braemar Iron Formation, 7 = Yamata Formation, 8 = Lake Khanka Formation, 9 = Rapitan Formation, 10 = Chuos Formation, 11 = Upper Tindir Group, 12 = Fulu Formation, 13 = Kingston Peak Formation, 14 = Numees Formation, 15 = Mugur Formation, 16 = Aok Formation, 17 = Corcoran and McMinn Formations, 18 = Mullera Formation, 19 = Chuanlinggou Iron Formation, 20 = Pike's Peak Iron Formation, 21 = Frere Formation, 22 = Alwar Group, 23 = Hutchison Group, 24 = Lake Superior region (includes five large iron formations), 25 = Sokoman Iron Formation, 26 = Shoshong Formation, 27 = Rochford Formation, 28 = Liaohe Group, 29 = Estes Formation, 30 = Pääkkö Iron Formation, 31 = Glen Township Formation, 32 = Lomagundi Group, 33 = Ijil Group, 34 = Hotazel Iron Formation, 35 = Timeball Hill Formation, 36 = Kursk Supergroup, 37 = Krivoy Rog Supergroup, 38 = Transvaal Province, 39 = Hamersley Province (includes six large iron formations), 40 = Cauê Formation, 41 = Penge Iron Formation, 42 = Benchmark Iron Formation, 43 = Nemo Iron Formation, 44 = Mulaingiri Formation, 45 = Nimba Itabirite, 46 = Atlantic City Iron Formation, 47 = Anshan, 48 = Caldeirão belt, 49 = Manjeri Iron Formation, 50 = Bababudan Group, 51 = Gimola terrane, 52 = Central Slave Cover Group, 53 = Carajás Formation, 54 = Olenegorsk Formation, 55 = Steep Rock Group, 56 = West Rand Group, 57 = Pongola Supergroup, 58 = Cleaverville Formation, 59 = Indian Creek Metamorphic Suite, 60 = Moodies Group.

Banded Iron Formations (very low O_2 in atm)

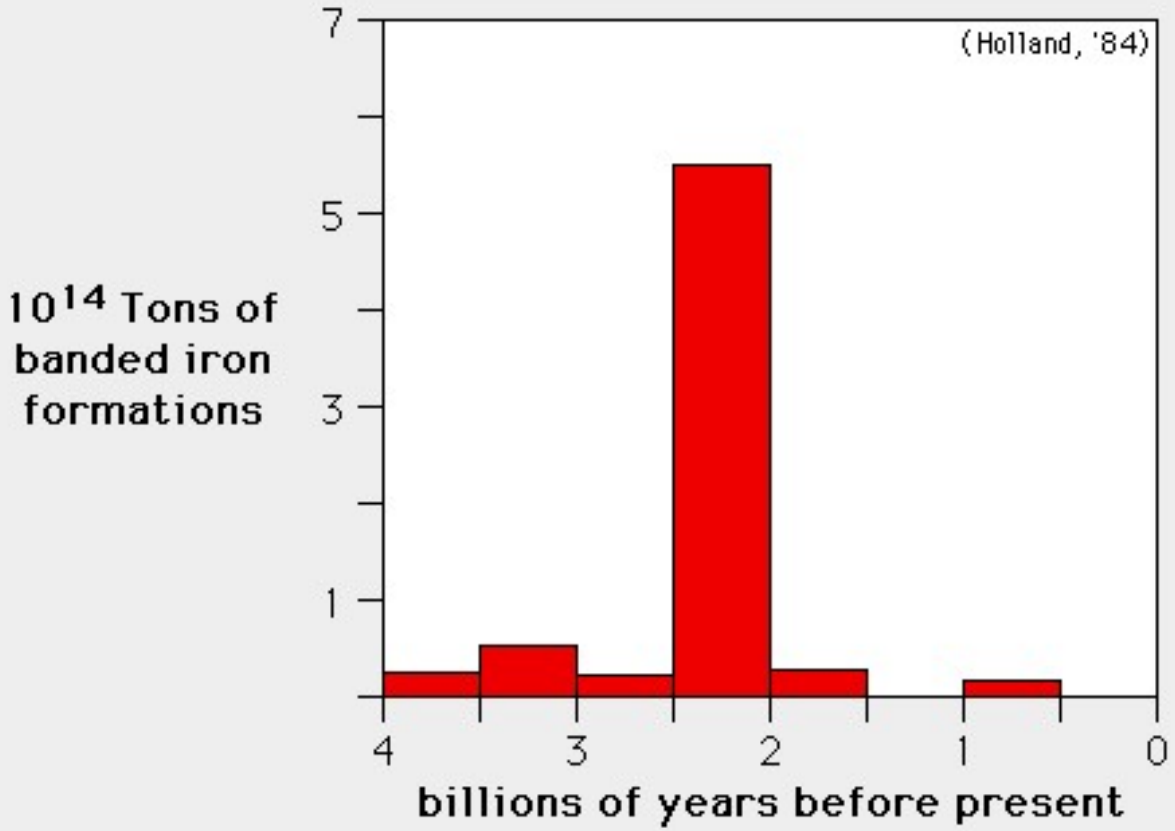

Very Large Fe Deposits

Continent	Area	Age (10^6 yrs)
Africa	Transvaal, S.A.	2100-2600
Australia	Hamersley Range	2400-2700
Eurasia	Krivoi Rog, Ukraine	1900-2600
North America	Labrador Trough, Canada	1900-2500
South America	Minas Gerais, Brazil	2000-2700

HJS/LP

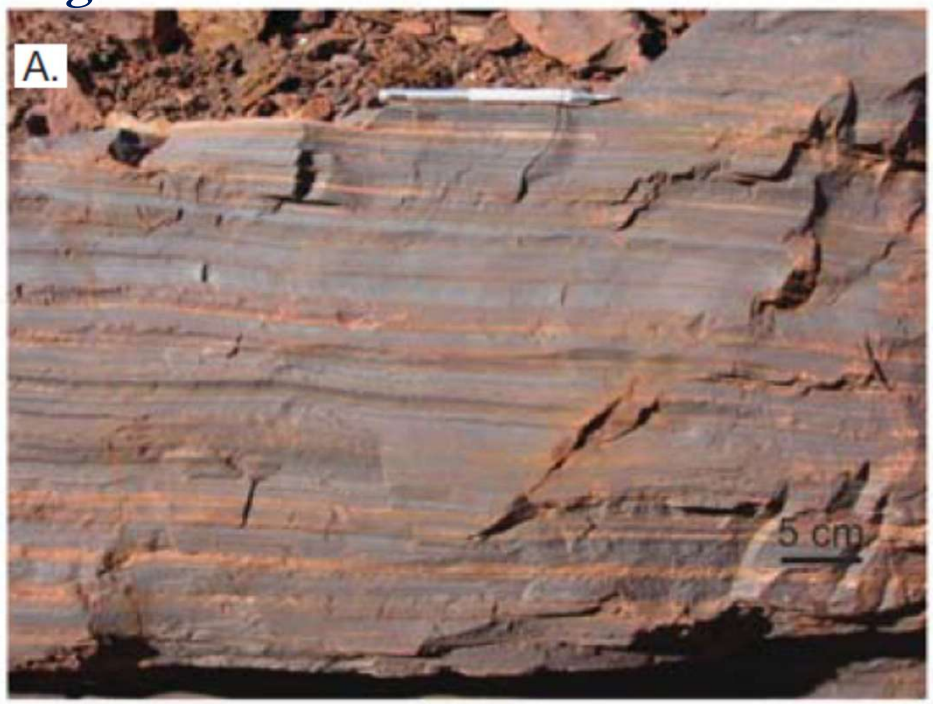

C.

10cm

Banding and compositional heterogeneity in BIF

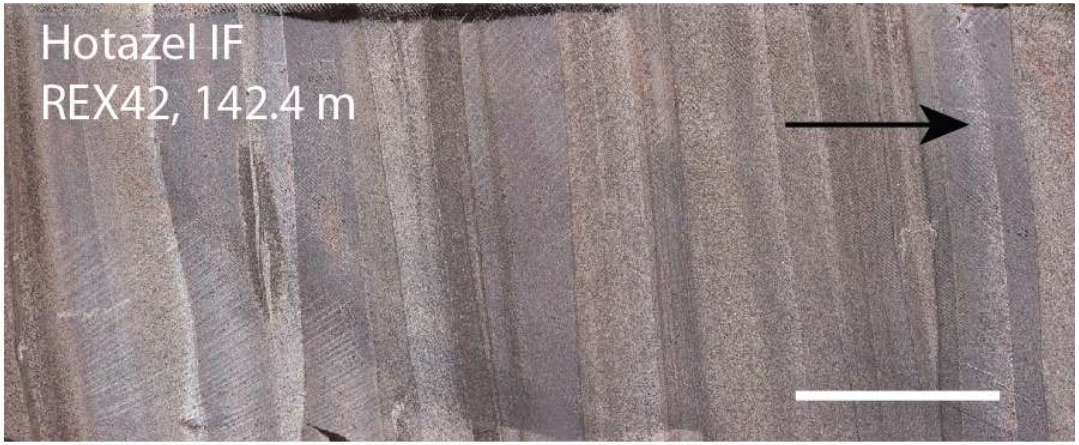

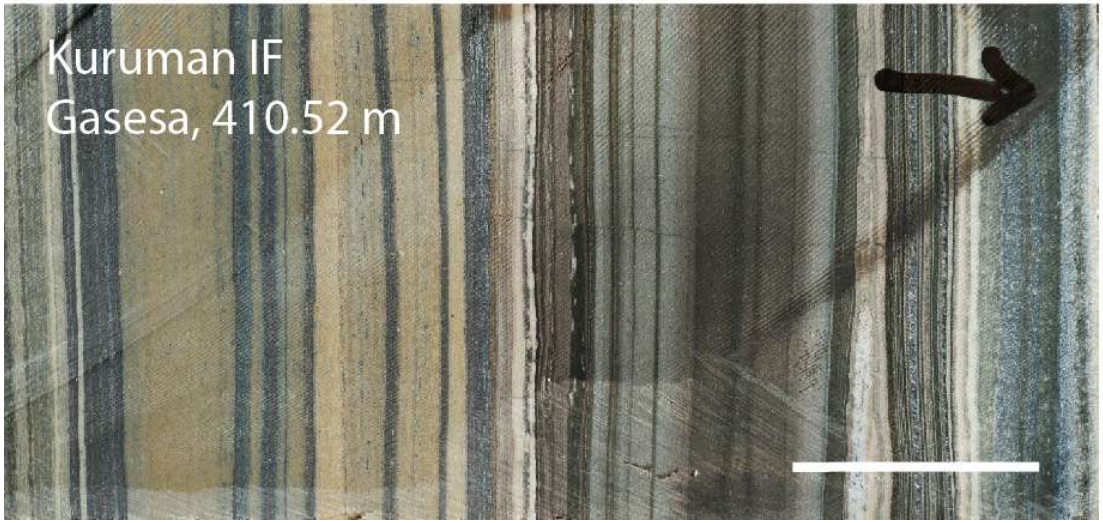

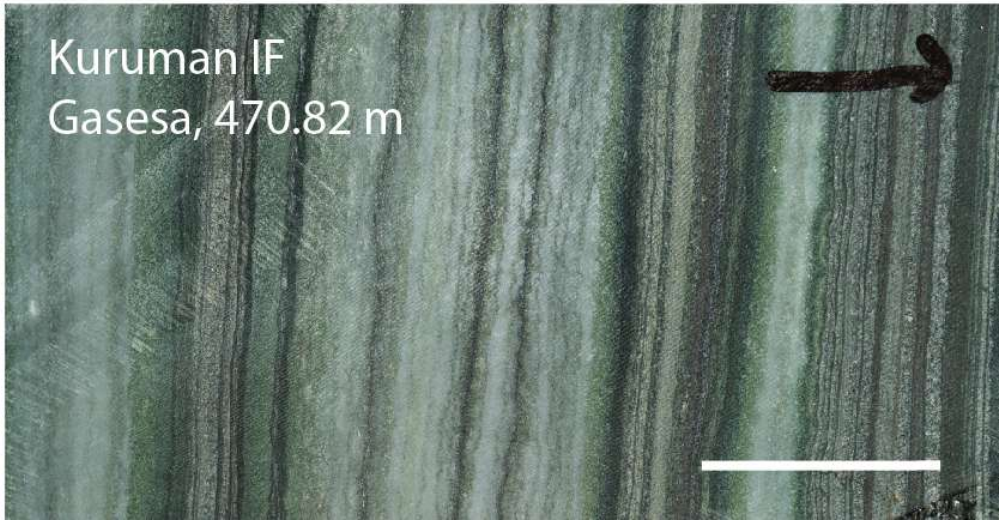

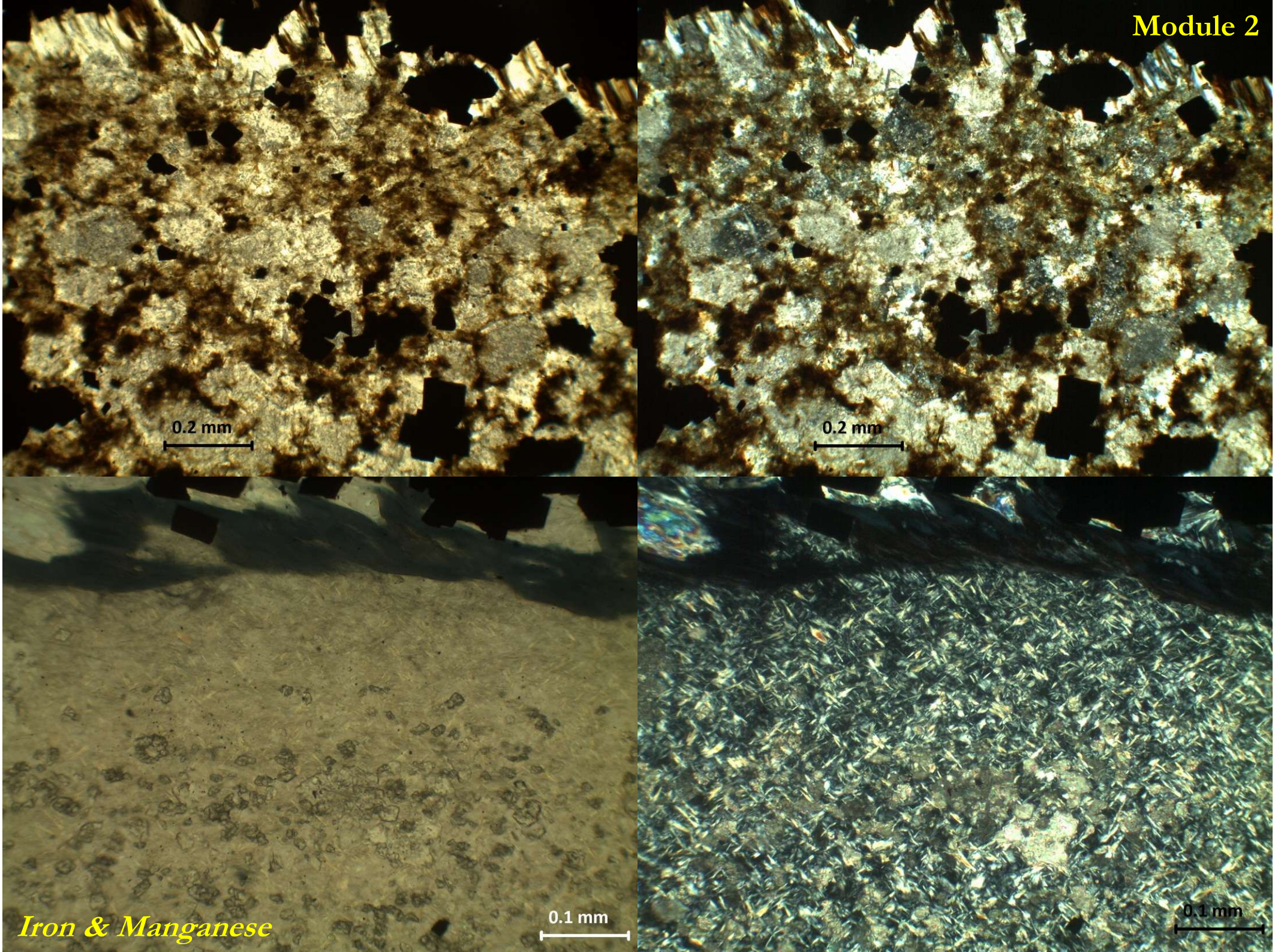
Module 2
0.2 mm
0.2 mm
Iron & Manganese
0.1 mm
0.1 mm

Silicate mineralogy in BIF

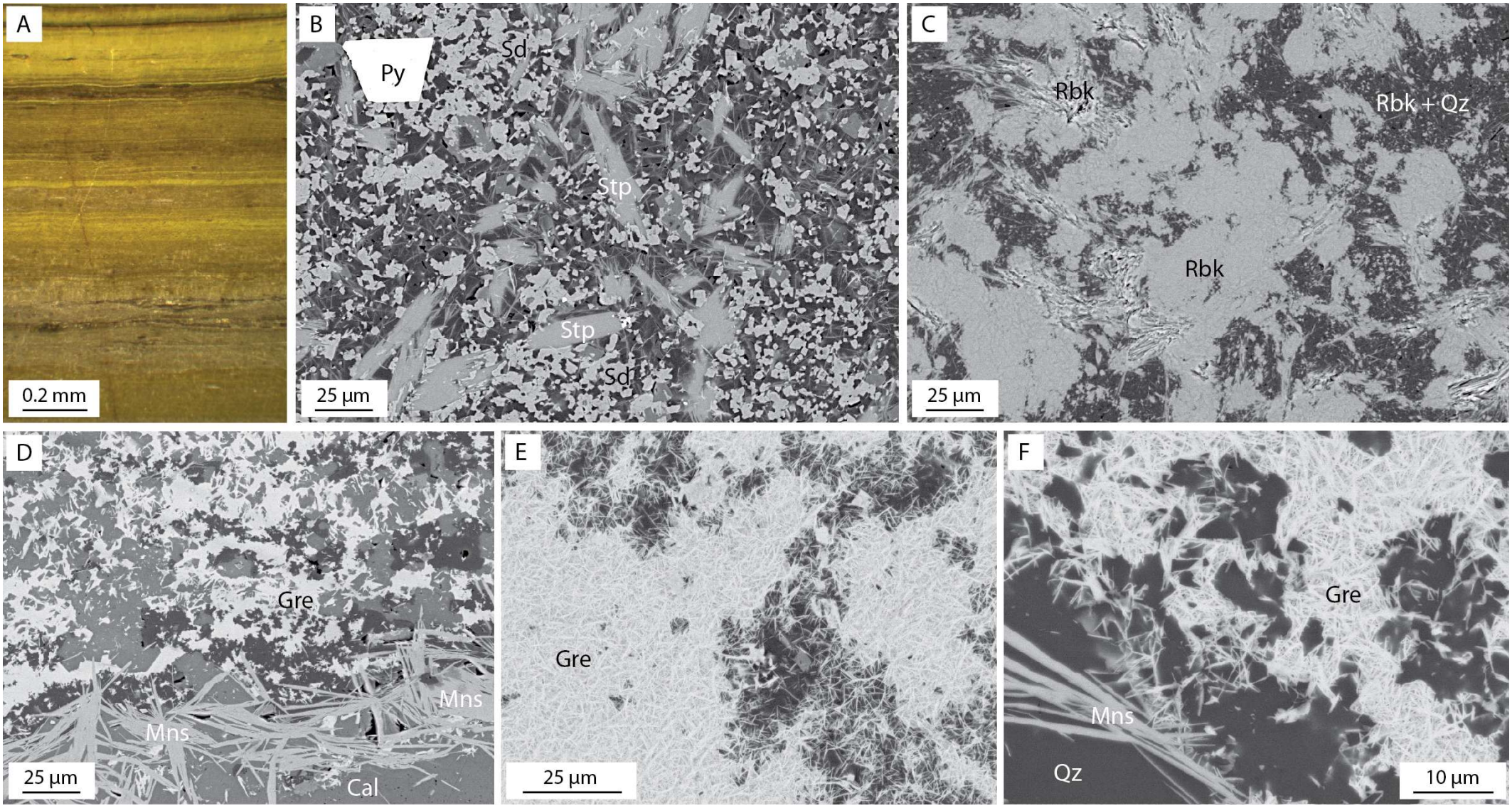

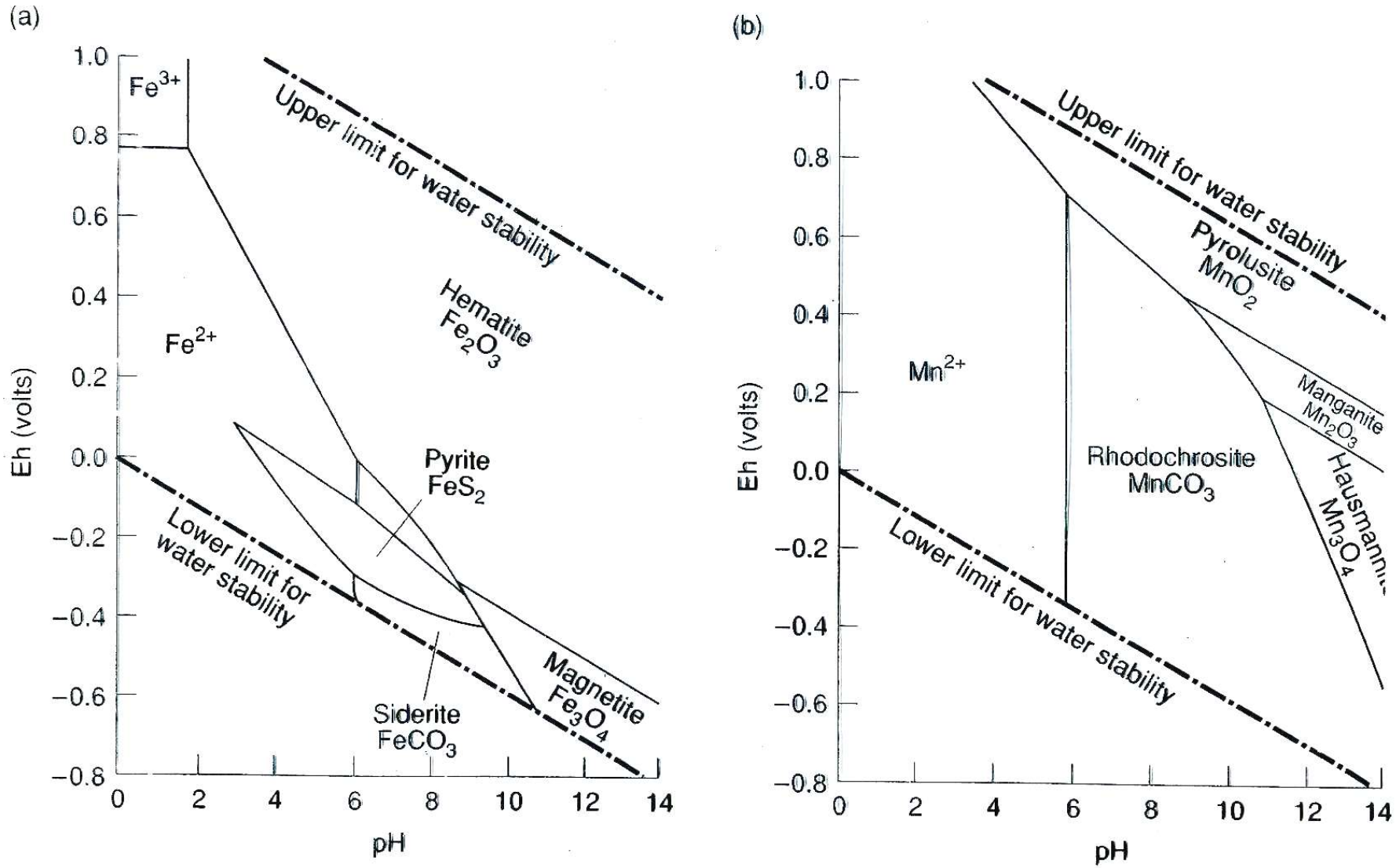

Figure 5.17 (a) Eh–pH diagram showing the stabilities of common iron minerals. The conditions that apply to this particular phase diagram are: T = 25 °C, P_{total} = 1 bar, molarities of Fe, S, and CO_3 are, respectively, 10^{-6}, 10^{-6}, and 1. (b) Eh–pH diagram showing the stabilities of common manganese minerals. Identical conditions apply, but with the molarity of Mn = 10^{-6} (diagrams modified after Garrels and Christ, 1965; Krauskopf and Bird, 1995). Note that the manganese oxides (MnO_2 and Mn_2O_3) are stable at higher Eh than the equivalent ferric oxide (hematite), and would only form, therefore, under more oxidizing conditions.

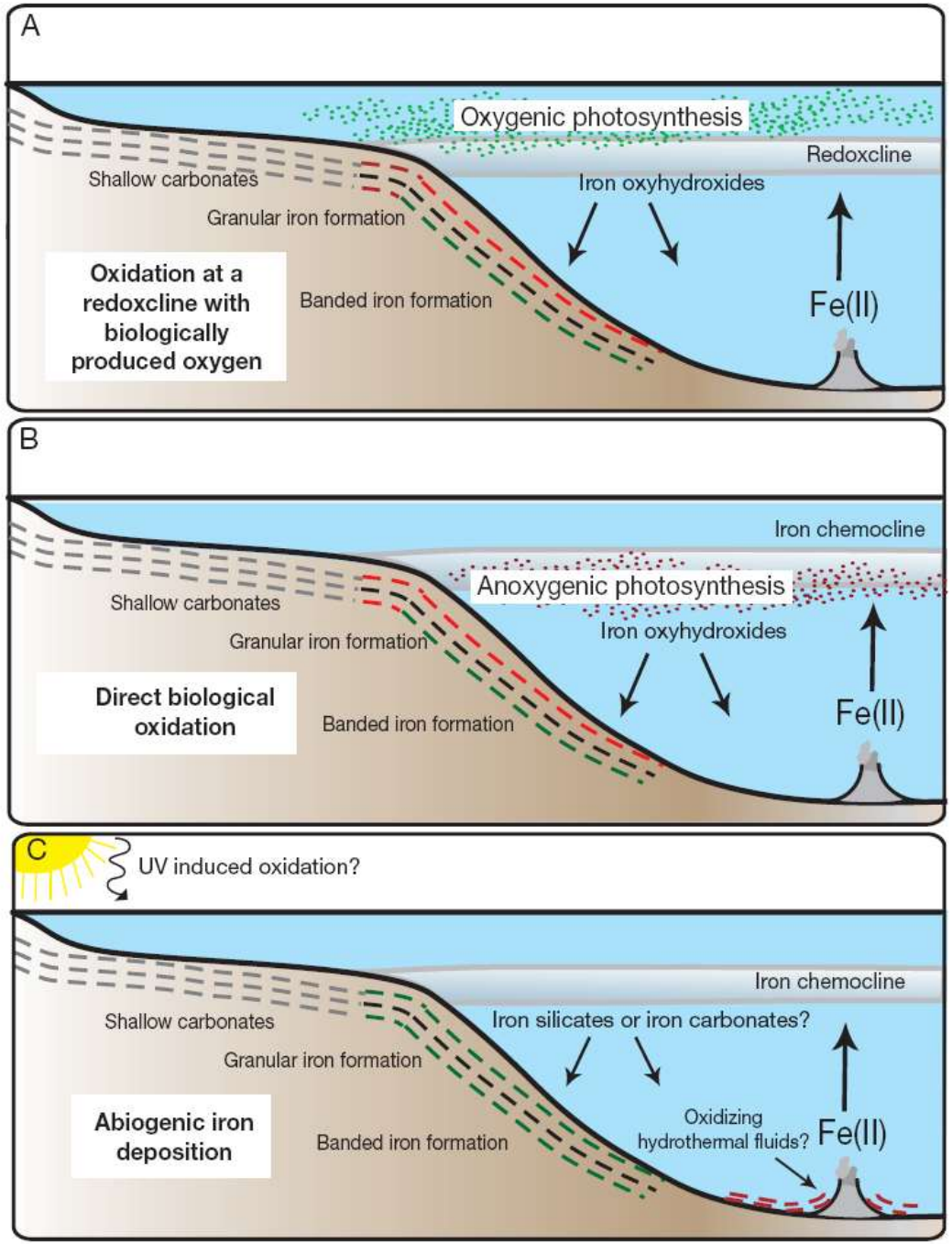

Simplified models for the deposition of Archean and Paleoproterozoic iron formations. Marked gradients in iron concentrations existed in both Archean and Proterozoic oceans in which iron-formation deposition occurred. Oxygen oases in shallow-water environments (A), above the redoxcline, generated by oxygenic photosynthesis were originally held responsible for deposition of iron formation (Cloud, 1973). However, during the Archean even shallow-water settings may have been reducing with respect to iron. In this case, it is unlikely that oxidation with dissolved divalent oxygen was an important process; anoxygenic photosynthesis (B) was probably the dominant means of ferrous iron oxidation. Photochemical oxidation of iron was also inferred (C) but is now considered insignificant.

Global distribution of major Mn deposits

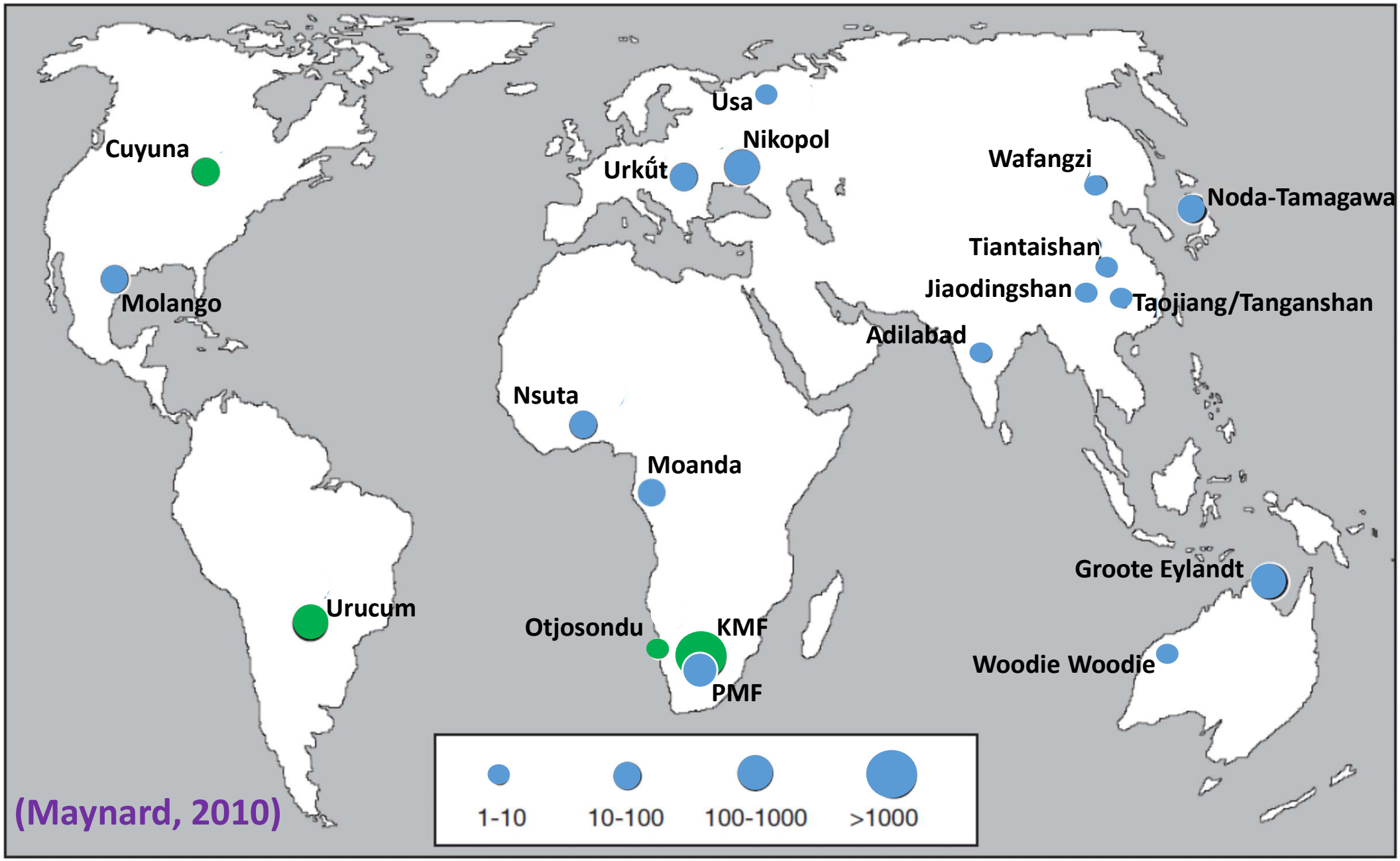

(Maynard, 2010)

Green circles: BIF association; Blue circles: carbonate/black shale association

The Transvaal Supergroup

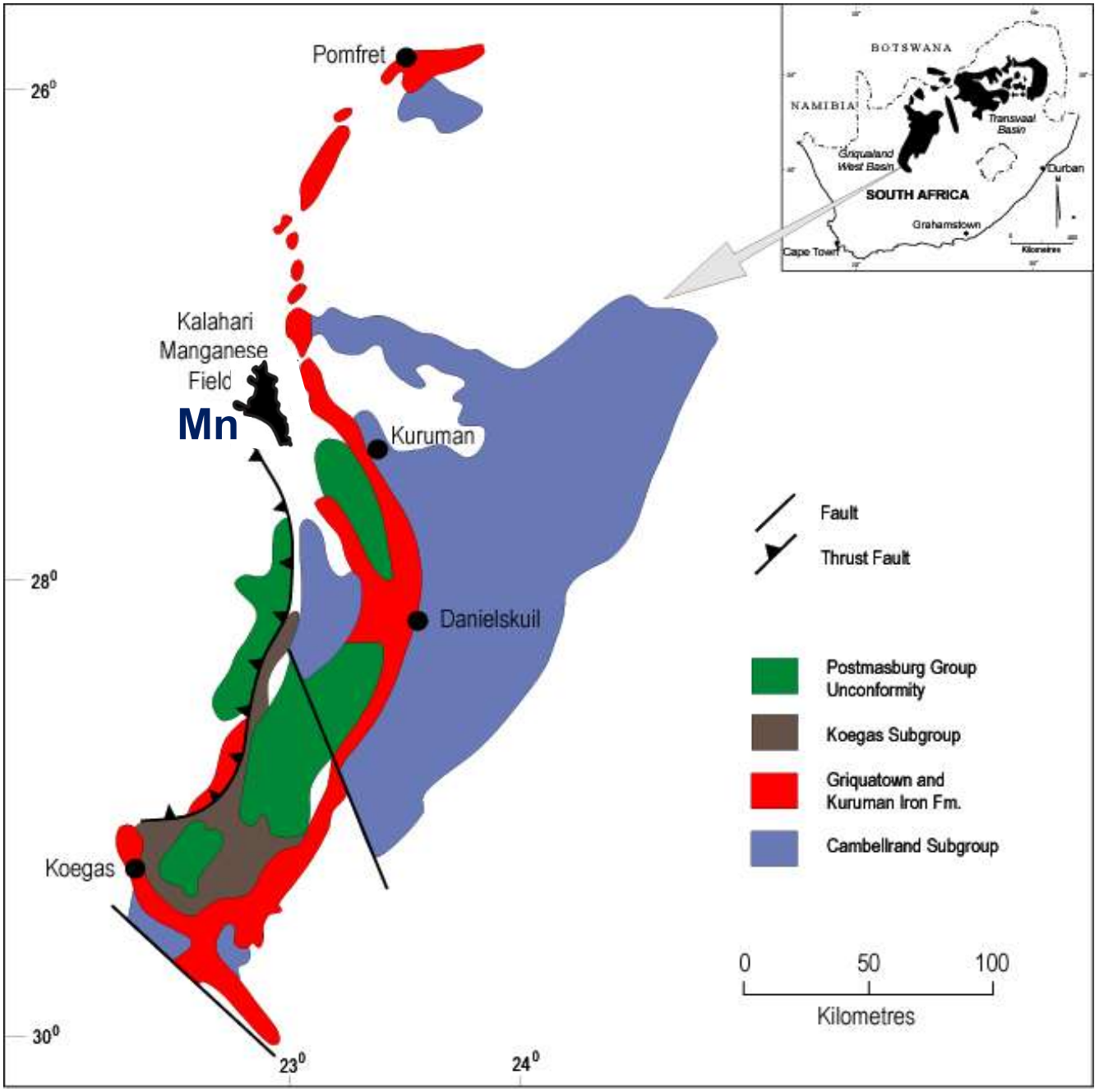

Stratigraphy

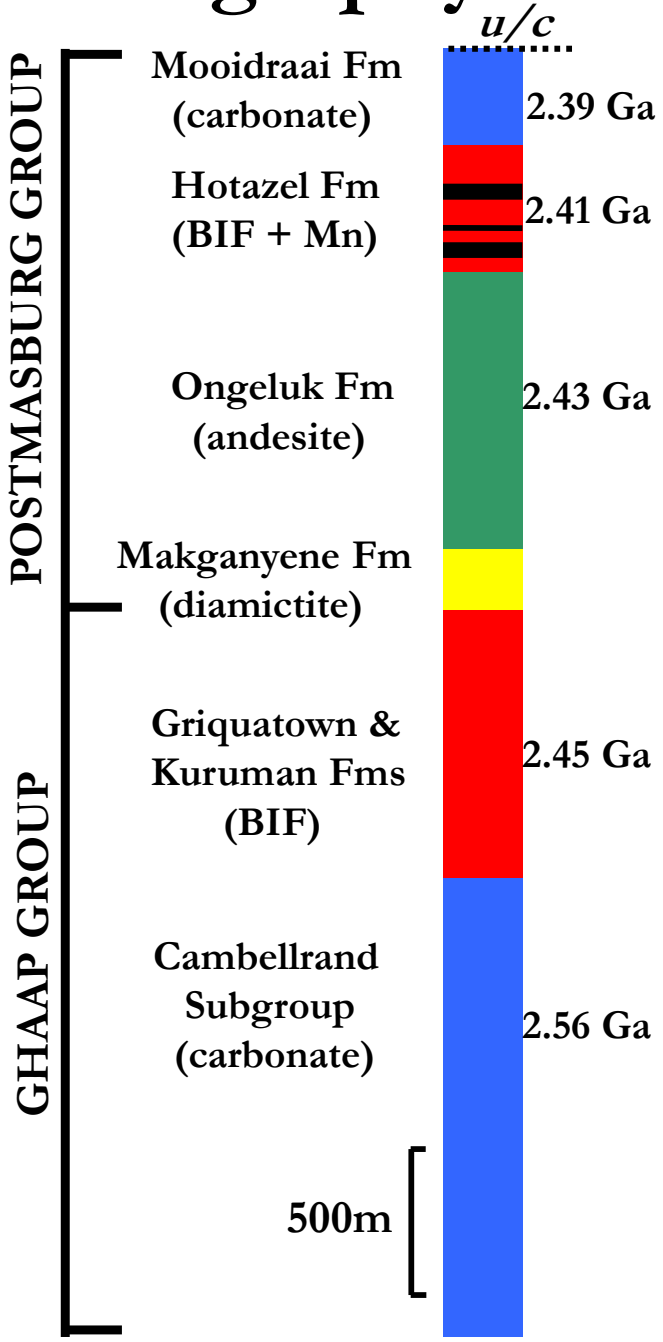

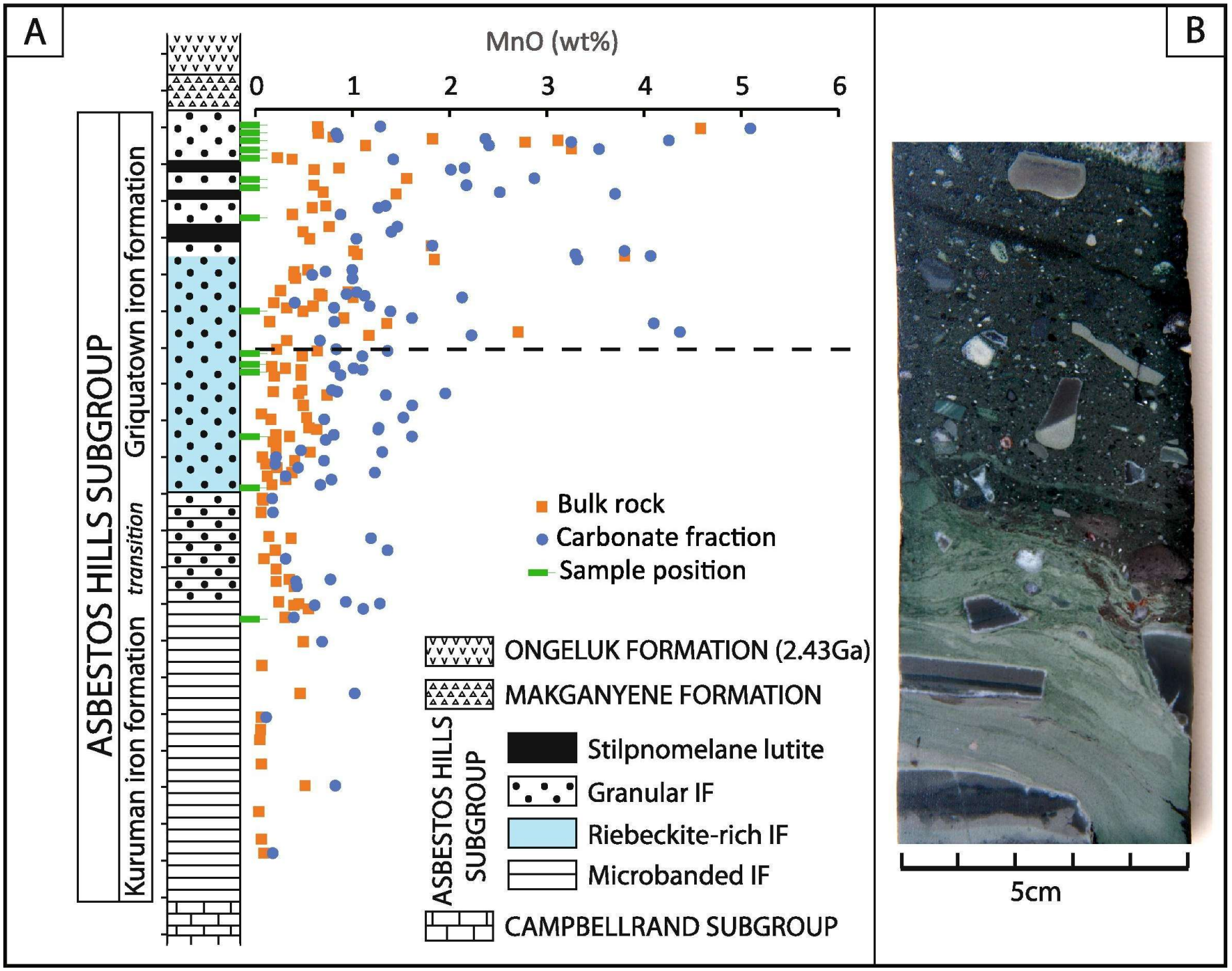
A
MnO (wt%)
0
1
2
3
4
5
6
ASBESTOS HILLS SUBGROUP
Griquatown iron formation
transition
Kuruman iron formation
Bulk rock
Carbonate fraction
Sample position
ONGELUK FORMATION (2.43Ga)
MAKGANYENE FORMATION
ASBESTOS HILLS SUBGROUP
Stilpnomelane lutite
Granular IF
Riebeckite-rich IF
Microbanded IF
CAMPBELLRAND SUBGROUP
B
5cm

The Kalahari Mn Field

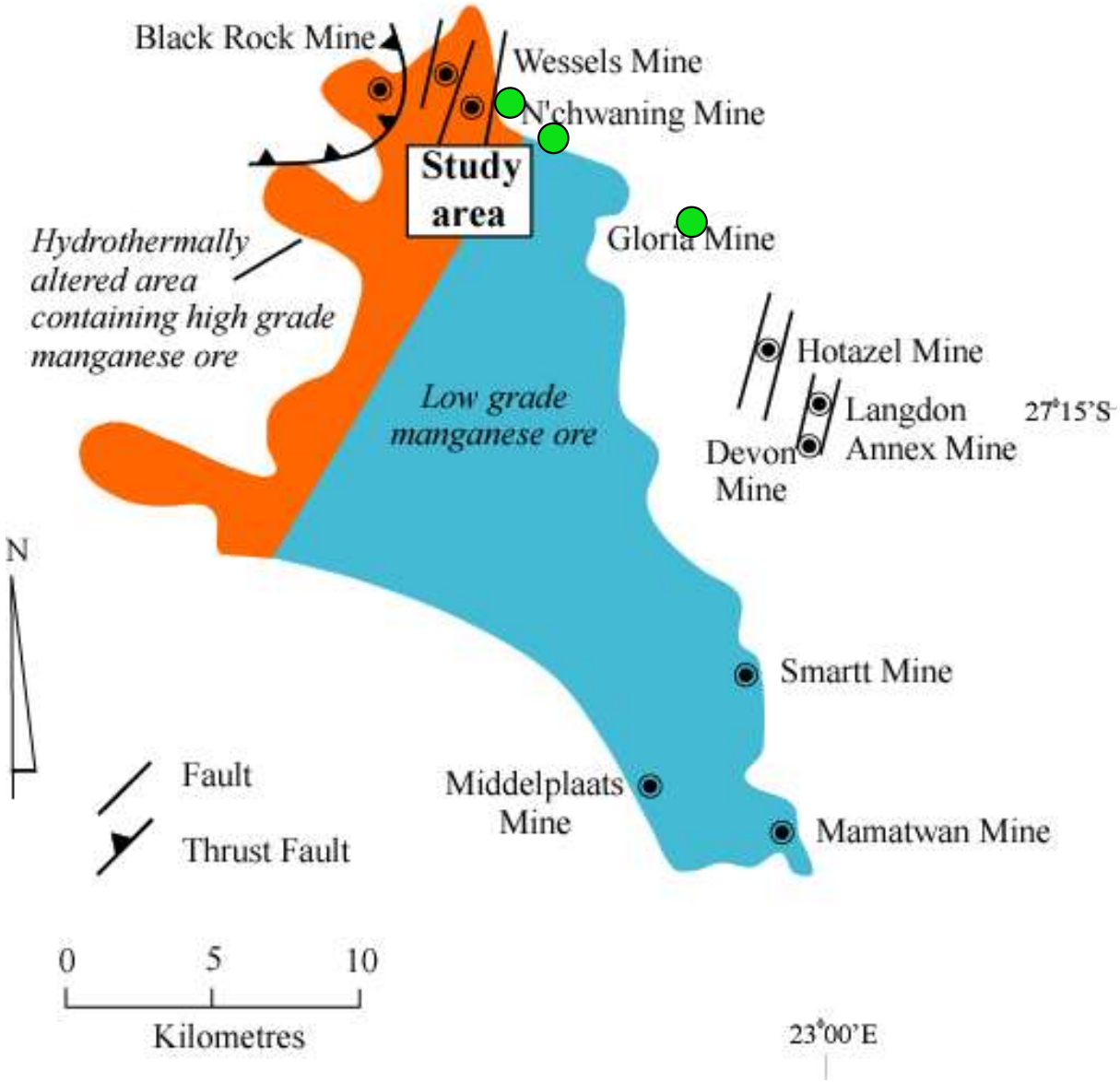

The Hotazel Fm

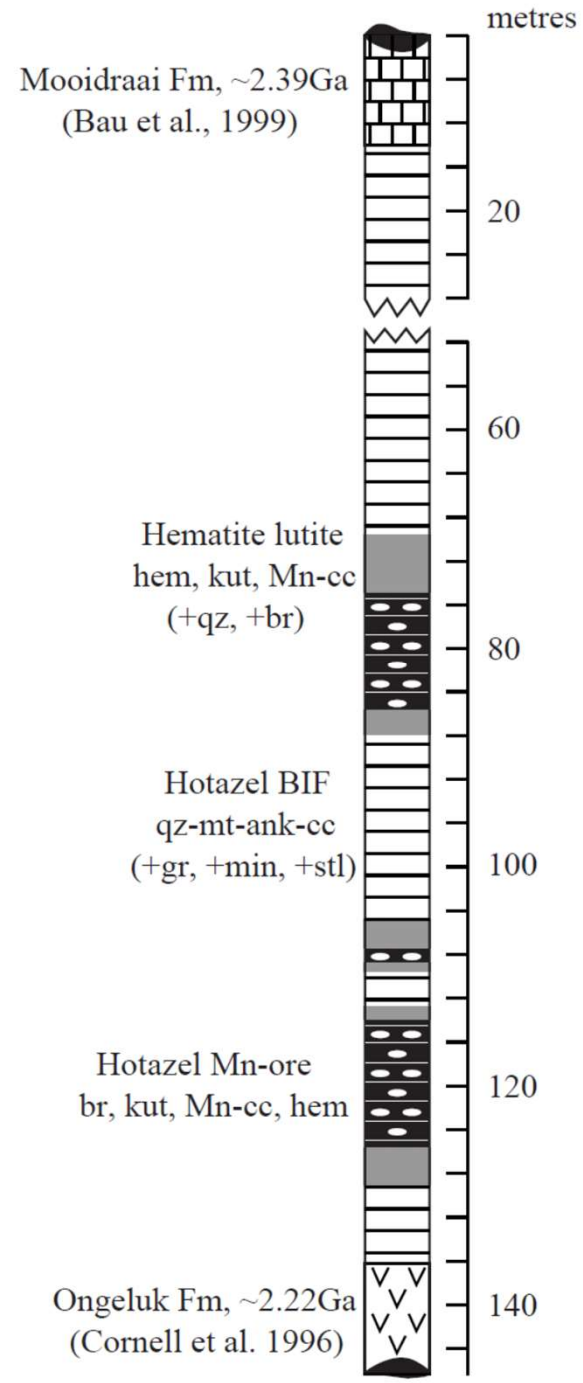


Iron & Manganese
Module 2

Chemical stratigraphy of the Hotazel Formation

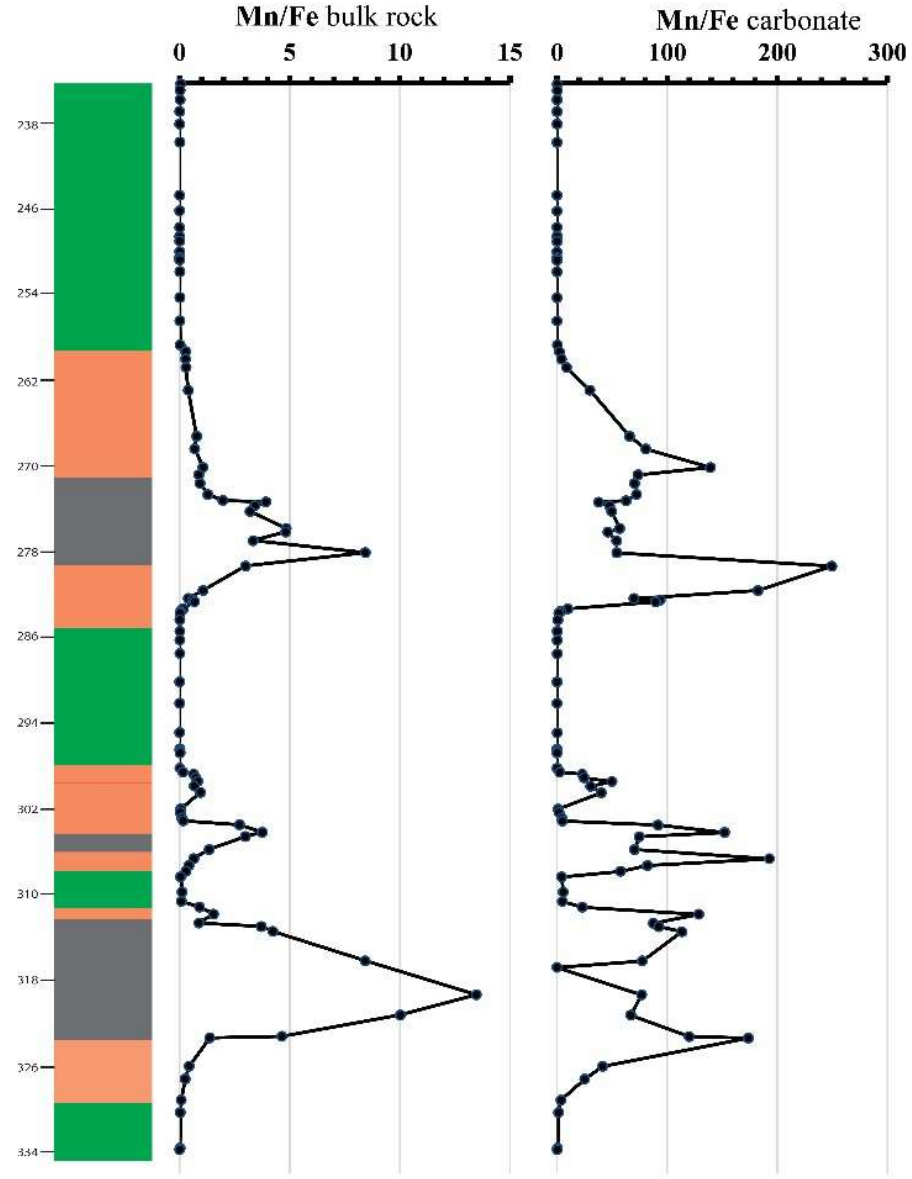

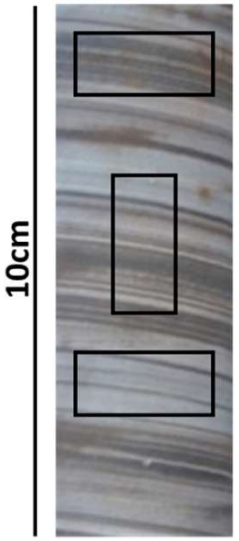

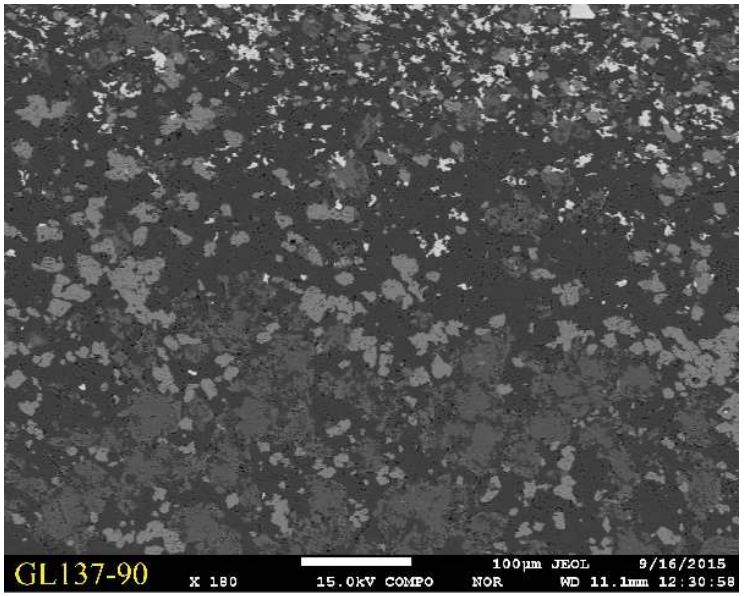

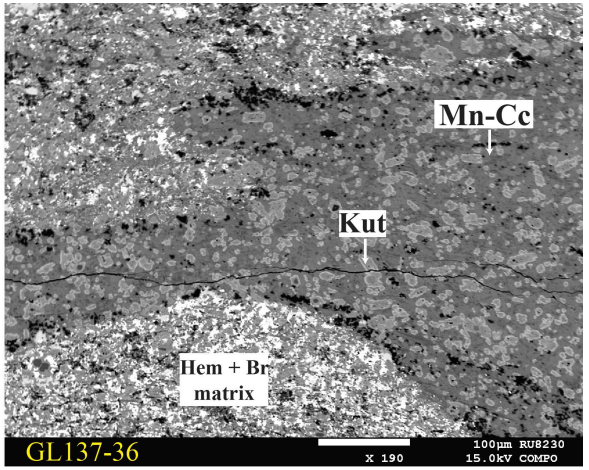

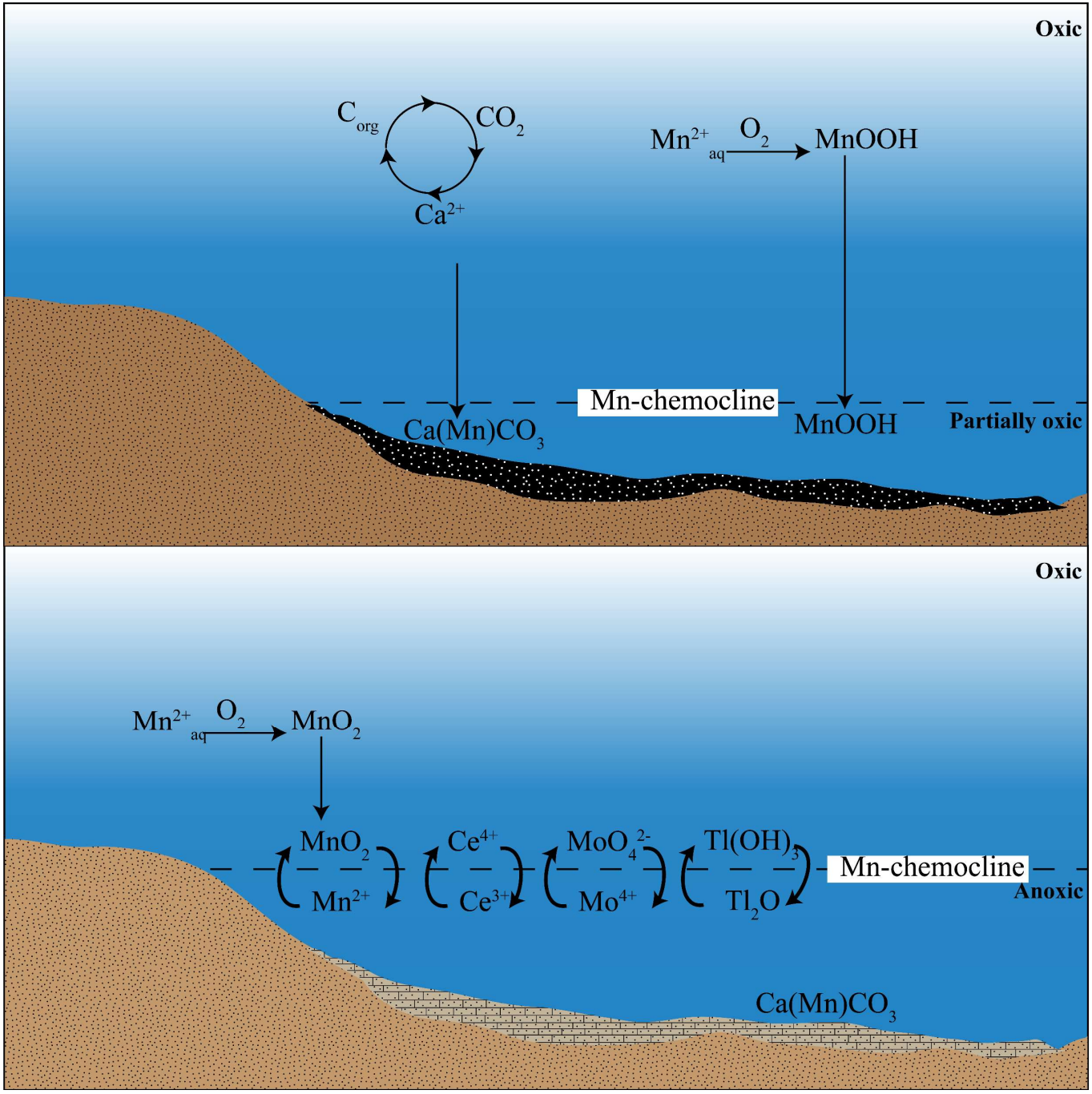
Oxic
C org
CO2
Ca2+
Mn2+ aq
O2
MnOOH
Mn-chemocline
Ca(Mn)CO3
MnOOH
Partially oxic
Oxic
Mn2+ aq
O2
MnO2
MnO2
Mn2+
Ce4+
Ce3+
MoO4 2-
Mo4+
Tl(OH)3
Tl2O
Mn-chemocline
Anoxic
Ca(Mn)CO3

Fe-Mn redox evolution and the GOE